Spectrochimica Acta Part A: Molecular and Biomolecular Spectroscopy 308 (2024) 123721

Contents lists available at ScienceDirect

Spectrochimica Acta Part A:
Molecular and Biomolecular Spectroscopy

journal homepage: www.journals.elsevier.com/spectrochimica-acta-part-a-molecular-and-biomolecular-spectroscopy

Fluorescence of *p*-hydroxyazobenzocrowns – Tautomeric equilibrium effect

Paulina Szulc [a], Elżbieta Luboch [a], Andrzej Okuniewski [b], Ewa Wagner-Wysiecka [a,c,*]

[a] Department of Chemistry and Technology of Functional Materials, Faculty of Chemistry, Gdańsk University of Technology, Narutowicza Street 11/12, 80-233 Gdańsk, Poland
[b] Department of Inorganic Chemistry, Faculty of Chemistry, Gdańsk University of Technology, Narutowicza Street 11/12, 80-233 Gdańsk, Poland
[c] Advanced Materials Center, Faculty of Chemistry, Gdańsk University of Technology, Narutowicza Street 11/12, 80-233 Gdańsk, Poland

HIGHLIGHTS

- *p*-Hydroxyazobenzocrowns have been characterized with spectroscopic methods.
- For the first time quantum yields values for *p*-hydroxybenzocrowns are given.
- Fluorescence properties are dependent on macrocycle size.
- Substituents in benzene rings affect the quantum yield values.

GRAPHICAL ABSTRACT

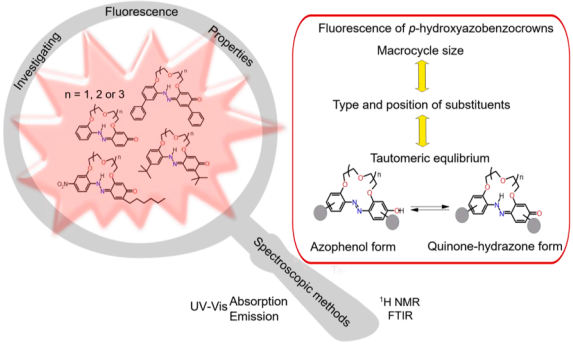

ARTICLE INFO

Keywords:
Azomacrocycles
Tautomerism
Hydrogen bond
Fluorescence

ABSTRACT

The spectroscopic properties of a series of *para*-hydroxyazobenzocrowns, including three novel compounds, were investigated using UV–Vis absorption and emission spectroscopy. This study presents, for the first time, determined quantum yield (QY) values for macrocycles of this category, ranging between 0.122 and 0.195. The highest values were obtained for crowns bearing two phenyl substituents in benzene rings. The impact of aromatic ring substituents and macroring size on the spectral characterization (^{1}H NMR and FTIR) of *p*-hydroxyazobenzocrowns was examined in consideration of the azophenol ⇄ quinone-hydrazone tautomeric equilibrium. Dipole moments of *p*-hydroxyazobenzocrowns in the ground and excited states have been determined. The alignment between experimental findings and theoretical studies was established.

1. Introduction

Azo compounds represent some of the earliest and most comprehensively understood synthetic organic compounds, continuing to be in high demand owing to their potential extensive applications across diverse fields in science, medicine, and industry [1]. Of particular interest are macrocyclic azo compounds, including those where the azo group is an integral component of the macrocycle [2]. Among them are azobenzocrowns - macrocyclic compounds in which azobenzene moiety is joined in 2,2′-positions with oligoether linkage. Azobenzocrowns were

* Corresponding author.
E-mail address: ewa.wagner-wysiecka@pg.edu.pl (E. Wagner-Wysiecka).

https://doi.org/10.1016/j.saa.2023.123721
Received 2 August 2023; Received in revised form 26 November 2023; Accepted 28 November 2023
Available online 1 December 2023

first obtained almost simultaneously, however on different synthetic ways, by Nakamura and coworkers in Japan [3,4] and in Biernat's group in Poland [5]. The integration of a chromogenic azo group and a macrocyclic complexation site within a singular molecule enables azobenzocrowns to function as chromophores, exhibiting a color change upon the complexation of a metal cation (with one nitrogen atom from the azo group acting as a donor atom). Macrocyclic site provides the discrimination of ions, among others, by their diameter. Since the first synthesis of azobenzocrowns many of their derivatives were obtained, studied and finally used as e.g. ionophores in ion-selective membrane electrodes (e.g. [6–11]) or/and were investigated as chromogenic ion receptors in solution (e.g. [6,8,12,13]).

The optical properties of azobenzocrowns are of particular interest among their features. Although much work has been done, there is still a gap in reports on their photoluminescent properties. It is because, in general, similarly to linear aromatic azo compounds [14,15], which are usually in the *trans* form, they do not show emission (with some exceptions). When emission is observed it is enhanced only for *cis* isomers [16,17]. Fluorescent are protonated forms of azo compounds [17,18]. The fluorescence of acyclic hydroxyazo compounds, which can exist in tautomeric forms as azophenol or quinone-hydrazone, has been extensively documented. Specifically, fluorescence is observed solely in the quinone-hydrazone forms [19–24].

In 1984, Kunitake and Simomure reported one such instance of fluorescent azo compounds, investigating azobenzene-containing bilayer membranes [25]. Additionally, Bisht et al. investigated the fluorescence properties of simple acyclic azo compounds, namely Methyl Orange and Direct Yellow 27, in solvents of varying polarities [26,27]. The relationship between the structure and fluorescence properties has been investigated for azo dyes when bound to tissues [28].

2-Borylazobenzenes bearing various substituents at the 4- and 4′-positions show intense yellow, green, orange, and red fluorescence [29]. It was stated that the stronger electron-donating group at the 4′-position the larger red shift of the π–π* absorption maximum and larger Stoke's shift. Additionally, the presence of a strong electron-donating group correlated with a higher fluorescence quantum yield. Interestingly, the optical properties of this category of azobenzenes appeared to be largely unaffected by the positioning of the electron-donating group.

An interesting example of unforeseen fluorescence in aromatic azo compounds was recently reported for macrocyclic derivatives by Hosgor and Akdag [30].

Given that fluorescence stands as a pivotal signal in domains like analytical chemistry [31,32], bioimaging [33], and others, the design, synthesis, and comprehension of fluorescence properties of azo compounds remain among the most compelling and pertinent research objectives [34]. The fluorescence characteristics of a system are undeniably influenced by structural factors. However, the chemical environment, particularly the solvent type and its polarity, can significantly impact the emission spectra of fluorophores and their quantum yields [35].

The fluorescence of acyclic hydroxyazo compounds, which may exist in tautomeric azophenol and quinone-hydrazone forms is fairly well documented in literature. In our prior studies, we highlighted the fluorescence of quinone-hydrazone forms of macrocyclic hydroxyazo compounds [6,18,37–39]: a series of macrocyclic *para*- and *ortho*-hydroxyazo compounds has been recently obtained and investigated in our group [6,8,12,13,18,36–39]. The general formulas of these compounds, comprising macrocycles where the azobenzene moiety is linked at 2,2′ positions by an oligoether chain, are depicted in Fig. 1. The investigation of the tautomeric equilibrium of these compounds revealed that *ortho*-hydroxy derivatives obtained so far predominantly exist in azophenol forms both in solution and in the solid state. Conversely, *para*-substituted derivatives tend to crystallize in the quinone-hydrazone tautomer [6,8,12,13,18,36–39]. Furthermore, our research demonstrated that the quinone-hydrazone form predominates

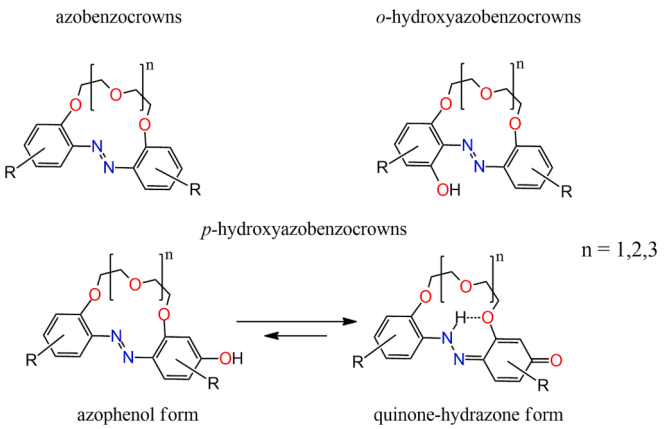

Fig. 1. The general formulae encompassing macrocyclic azo compounds—azobenzocrowns and *ortho*-hydroxyazobenzocrowns—as well as the tautomeric equilibrium exhibited by *para*-hydroxyazobenzocrowns.

in many cases in organic solvent solutions. Notably, the equilibrium between tautomers was found to be influenced by macrocycle size, the presence of ionic species (such as metal cations, acids, or bases), and the type of solvent.

The objective of this study is to explore the correlation between the structure of *p*-hydroxyazobenzocrowns (including macroring size and the impact of substituents in benzene rings) and their spectral properties, specifically fluorescence. This investigation aims to establish a groundwork for utilizing this relationship in the future design of efficient fluorogenic molecules.

2. Results and discussion

Until now, the quantitative investigation of the emission properties of *p*-hydroxyazobenzocrowns has been lacking. This study marks the first comprehensive examination of the fluorescence characteristics of *p*-hydroxyazobenzocrowns, establishing a correlation between chemical structure and quantum yield. To achieve this, macrocycles of various sizes (13-, 16-, and 19-membered) and differing types and positions of substituents in the benzene rings were used (Fig. 2).

2.1. Synthesis

The synthesis of the majority of the macrocycles studied in this work followed previously described procedures by our group [6,8,12,13,18,36–39]. Among them, compound **I**, di-Ph-19-*p*-OH (Fig. 2), previously obtained via a photochemical rearrangement [39], was newly synthesized using a reaction analogous to the Wallach rearrangement (Scheme S1). This synthetic route was pursued for comparative purposes with previously studied cases. Despite being more labor-intensive and less environmentally friendly, this method exhibited a higher yield of transformation compared to the photochemical rearrangement. Notably, in the photochemical reaction conducted in propan-2-ol, this macrocycle was obtained with a yield of 31.6 % [39], while in Wallach's rearrangement it was obtained with a yield of 49%.

Three of the macrocycles—di-*t*-Bu-13-*p*-OH (**D**), di-*t*-Bu-16-*p*-OH (**E**), and NO2-C6-19-*p*-OH (**L**)—are novel compounds previously unreported in the literature. The synthetic approach is shown in Scheme S1 and detailed synthetic procedures are provided in the Supplementary Material. The influence of substituents on the resultant products and their respective ratios in the photochemical rearrangement processes was discussed in [39].

The synthesis of compound **L** followed the Williamson protocol as in previously described procedure [13]. The yield of macrocyclization appeared to be linked to the macrocycle's size. Compounds **J** and **K**, with 13- and 16-membered rings, were obtained via this method with yields

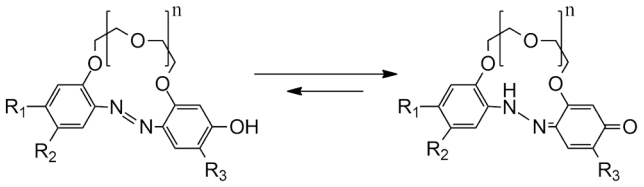

n = 1	n = 2	n = 3
A. R_1=R_2=R_3=H	B. R_1=R_2=R_3=H	C. R_1=R_2=R_3=H
D. R_1=H, R_2=R_3=*t*-Bu	E. R_1=H, R_2=R_3=*t*-Bu	F. R_1=H, R_2=R_3=*t*-Bu
G. R_1=H, R_2=R_3=C_6H_5	H. R_1=H, R_2=R_3=C_6H_5	I. R_1=H, R_2=R_3=C_6H_5
J. R_1=NO_2, R_2=H, R_3=*n*-C_6H_{13}	K. R_1=NO_2, R_2=H, R_3=*n*-C_6H_{13}	L. R_1=NO_2, R_2=H, R_3=*n*-C_6H_{13}

Fig. 2. The tautomeric equilibrium of *p*-hydroxyazobenzocrowns with varying sizes of the macrocycle and different types and positions of substituents in the benzene rings.

of 10 % and 7 %, respectively [13]. However, the 19-membered macrocycle (compound **L**) was obtained with a yield of 2 %. The structure of newly obtained compounds was confirmed by spectroscopic methods. The respective spectra are included in Supplementary Material.

2.2. Spectral characterization of p-hydroxyazobenzocrowns

The molecular structures of the quinone-hydrazone (QH) forms of all investigated *p*-hydroxyazobenzocrowns **A**-**L** are shown in Table 1. In current research *p*-hydroxyazobenzocrowns featuring unsubstituted benzene rings, namely macrocycles of 13-, 16- and 19-membered rings (compounds **A**, **B**, **C**) serve as reference compounds to which the properties of their substituted analogs are compared. Next group of macrocycles consists of the symmetrical derivatives bearing two substituents in *para* positions to oligoether moiety, namely alkyl (*t*-Bu: compounds **D**, **E** and **F**) or aryl (Ph: compounds **G**, **H** and **I**). The third group comprises macrocyclic azo compounds in which two different substituents, namely nitro- (*meta* to oligoether moiety, *para* to azo group) and *n*-hexyl (*para* to oligoether moiety) groups, are located in adjacent benzene rings (compounds **J**, **K** and **L**).

In previous studies we have demonstrated that the tautomeric equilibrium of *p*-hydroxyazobenzocrowns depends on various factors, including the macrocycle size, the type of substituents in benzene rings. Additionally tautomeric equilibrium is influenced by the concentration

Table 1
The contribution of quinone-hydrazone (QH) tautomer of *p*-hydroxyazobenzocrowns in acetonitrile (results from ^{1}H NMR measurements at concentration of macrocycles ~ 10^{-2} M).

Macrocycle size	Formula and the contribution of quinone-hydrazone tautomer			
13-membered	A. 13-*p*-OH	D. di-*t*-Bu-13-*p*-OH	G. di-Ph-13-*p*-OH	J. NO2-C6-13-*p*-OH
	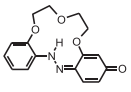	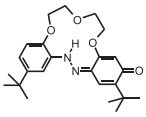	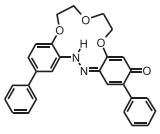	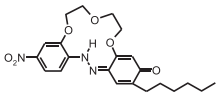
	100 % [37]	100 % [this work]	100 % [6]	100 % [this work]
16-membered	B. 16-*p*-OH	E. di-*t*-Bu-16-*p*-OH	H. di-Ph-16-*p*-OH	K. NO2-C6-16-*p*-OH
	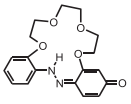	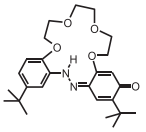	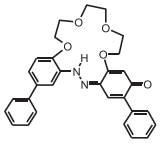	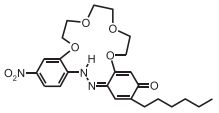
	100 % [37]	100 % [this work]	100 % [6]	100 % [this work]
19-membered	C. 19-*p*-OH	F. di-*t*-Bu-19-*p*-OH	I. di-Ph-19-*p*-OH	L. NO2-C6-19-*p*-OH
	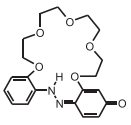	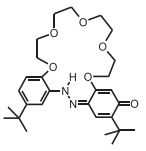	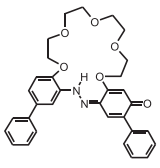	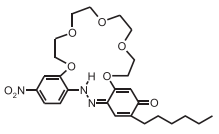
	25 % [37]	90 % [38]	77 % [39]	58 % [this work]

and the type of the solvent [cf. [37,38]]. The plausible mechanism of quinon-hydrazone-azophenol tautomerization is presented in Supplementary Material (Fig. S40). It was found that in acetonitrile for the majority of the investigated *p*-hydroxyazobenzocrowns tautomeric equilibrium is, in most cases, shifted towards quinone-hydrazone form. This rule is also obeyed for newly synthetized macrocycles namely compounds **D** and **E**, with the well observable across the series of macrocycles the reduction of the contribution of quinone-hydrazone form for 19-membered ring compounds. This characteristic is also evident for compounds **J-L**, which have not previously been investigated so far in this aspect. Worth noting is also the comparison of the influence of the effect of the substituents in benzene rings on the quinone-hydrazone equilibrium of 19-membered macrocycles. The steric effect of the *m*-substituents (to azo group) is observed to stabilize the quinone-hydrazone tautomer. In Table 1 the contribution of the quinone-hydrazone form (QH) for compounds **A-L** determined on the basis of ^{1}H NMR (see Supplementary Material) in acetonitrile is listed. In acetonitrile, spectra of 13- and 16-membered macrocycles show only one set of proton signals indicative to the quinone-hydrazone tautomer. In spectra of 19-membered crowns double set of signals is observed reflecting the presence of both tautomeric forms under spectra registration conditions. The most characteristic signal for quinone-hydrazone tautomer is singlet typically positioned between 5–6 ppm, corresponding to proton at *ortho*-position to oligoether linkage in quinone ring. ^{1}H NMR spectra this group of compounds were analyzed in details in previous studies [cf. [37–39]]. For further studies in solution in this research we used acetonitrile.

Firstly, UV–Vis and fluorescence spectra of *p*-hydroxyazobenzocrowns were recorded in acetonitrile to investigate the influence of macrocycle size and substituents on the absorption and emission spectra. Table 2 consolidates the spectral characteristics: including the position of longwave absorption band, molar absorption coefficient values, emission maximum position, quantum yield values and the Stokes shift for compounds **A-L**.

UV–Vis absorption spectra of the investigated series of *p*-hydroxyazobenzocrowns were registered in acetonitrile and all of them are shown in Supplementary Material. Generally, the absorption spectra of hydrazones exhibit a bathochromatic shift in comparison to their corresponding azo tautomers [41,42] which is also observed for *p*-hydroxyazobenzocrowns [37–39]. The position of absorption band of quinone-hydrazone form of *p*-hydroxyazobenzocrowns typically falls within 430–450 nm range, whereas azophenol tautomers absorb at ~ 350 nm. The tautomeric equilibrium is dependent on the macrocycle size, the type of substituent(s) and the properties of solvent [37–39].

It is well known that for azobenzene derivatives the position of absorption maxima is primarily influenced by the substituent in the *para* position to azo group [24,43–45]. Substituents in *ortho* or *meta* positions usually have a lesser or negligible effect on the spectral properties. In fact, the presence of electron donating *t*-Bu groups in *the meta* position to azo group causes a minor shift of absorption band of *p*-hydroxyazobenzocrowns towards lower energy levels, which is observed as bathochromic shift of absorption band (+6 nm for **D** and **E** and + 8 nm for **F**). This is apparent when comparing the position of the longwave band in the spectra of unsubstituted *p*-hydroxyazobenzocrowns (**A-C**).

This rule is similarly observed for diphenyl derivatives **G-I**, displaying a red shift in the absorption maximum by 18, 16, and 19 nm, respectively, when compared to the position of the absorption band in unsubstituted crowns **A-C**. The greater shift observed in diphenyl derivatives compared to t-Bu-bearing macrocycles can be attributed to the resonance effect of the phenyl substituent. Phenyl substituents can adopt a planar arrangement, which enhances their donor potential. This results in the more pronounced bathochromic shift of the absorption band [46].

The presence of electron-withdrawing nitro group in the *para* position to the azo moiety intensifies the delocalization within the conjugated system in compounds **J-L** and is the cause of the bathochromic shift (+20 nm for **J** and + 18 nm for **K** and **L**) of absorption band, when compared to their unsubstituted analogs. The effect of substituents on

Table 2
Spectral characteristics of macrocycles **A-L**, azobenzene and *p*-hydroxyazobenzene in an acetonitrile.

Compound/ring size/substituents	Absorption	Emission band*		Stoke's shift** [nm]	Stoke's shift [cm^{-1}]
	λ_A [nm](ε) [dm^3·mol^{-1}·cm^{-1}]	$\lambda_{E(max)}$ [nm]	QY		
A. 13-*p*-OH	432 ($2.31\cdot10^4$)	526	0.158	94	4137
B. 16-*p*-OH	432 ($2.05\cdot10^4$)	534	0.138	102	4422
C. 19-*p*-OH	434 ($1.60\cdot10^4$)	536	0.128	102	4385
D. di-*t*-Bu-13-*p*-OH	438 ($8.09\cdot10^3$)	540	0.151	102	4313
E. di-*t*-Bu-16-*p*-OH	438 ($1.92\cdot10^4$)	544	0.147	108	4449
F. di-*t*-Bu-19-*p*-OH	442 ($3.19\cdot10^4$)	546	0.146	104	4309
G. di-Ph-13-*p*-OH	450 ($3.20\cdot10^4$)	556	0.195	106	4237
H. di-Ph-16-*p*-OH	448 ($2.60\cdot10^4$)	560	0.186	112	4464
I. di-Ph-19-*p*-OH	453 ($2.87\cdot10^4$)	562	0.183	111	4281
J. NO2-C6-13-*p*-OH	452 ($3.20\cdot10^4$)	514	0.146	62	2669
K. NO2-C6-16-*p*-OH	450 ($3.65\cdot10^4$)	514	0.128	64	2767
L. NO2-C6-19-*p*-OH	452 ($9.32\cdot10^3$)	512	0.122	60	2593
azobenzene [14]	316 ($2.24\cdot10^4$)	nd	nd	nd	nd
p-hydroxyazobenzene [40]	345 ($2.04\cdot10^4$)	390	nd	45	3345

* Excitation at wavelength of absorption maximum; nd – no data.
** Stokes' shift (λ_A- $\lambda_{E(max)}$) given in relation to the long wavelength maximum of QH-form.

the position of absorption band regarding macrocycles of the same ring size, is demonstrated in Fig. 2 by absorption spectra of 19-membered crowns (solid lines).

Evident fluorescence, as it is often found for azo compounds existing in quinone-hydrazone form [47], is also observed for all of investigated macrocycles **A-L** in acetonitrile. The position of emission band for the *p*-hydroxyazobenzocrowns is illustrated using the spectra of 19-membered macrocycles **C**, **F**, **I**, **L** in Fig. 3 (dashed lines). Complete data for all the macrocycles studied herein are collected in Table 2 and are included in Supplementary Material. It suggests a little dependence of the position of emission maxima on the size of the macrocycle when comparing *p*-hydroxyazobenzocrowns with the same type of substituents. Furthermore, the emission spectra are influenced by the type and the position of substituents in benzene rings (Fig. 3). An interesting trend is observed in the Stoke's shifts (Fig. 4a). Namely, the most significant difference between the positions of the absorption and emission maxima is observed consistently for the 16-membered macrocycles (**B**, **E**, **H** and **K**) regardless of the substituent types. This may correlate with the alterations in the molecule flexibility attributed to the length of the oligoether linkage, which can affect the planarity of the molecules. The lowest Stoke's shift exhibit macrocycles **J-L** bearing electron withdrawing nitro group. Another interesting relationship was found for quantum yield values (Fig. 4b). The primary influencing factor appears to be the size of the macrocycle. When comparing the quantum yield values of the unsubstituted *p*-hydroxyazobenzocrowns **A-C**, it becomes evident that the quantum yield value decreases with increasing size of the macroring. This trend is observed across all investigated macrocycles, regardless of the type of substituents.

In our earlier studies we have established the dependency of the tautomeric equilibrium *p*-hydroxyazobenzocrowns on various factors including among the others the macrocycle size [37,38]: generally the smaller macrocycle the greater the tendency to exist in quinone-hydrazone tautomer. One of the factors contributing to stabilization of the quinone-hydrazone form appears to be a presence of intramolecular hydrogen bond N-H···O (cf. Fig. 1 and Fig. 5). Spectroscopic methods such as NMR and FTIR spectroscopy can be useful tools in investigation of the hydrogen bonded systems [48–50]. In ^{1}H NMR of the *p*-hydroxyazobenzocrowns the low-field shift of N–H proton signal can be used for the estimation of the hydrogen bonding system. The positions of the N–H proton signal in ^{1}H NMR spectra of compounds **A-L** registered in acetonitrile-d_3 are collected in Table 3. The effect of the macrocycle size is exemplified with partial ^{1}H NMR spectra of compounds **A-C** (acetonitrile-d_3) in Fig. 5 (left). Additionally, in Fig. 5 (right) the relationship between the macrocycle size and the position of N–H proton signal in ^{1}H NMR spectra of compounds **A-L** is shown.

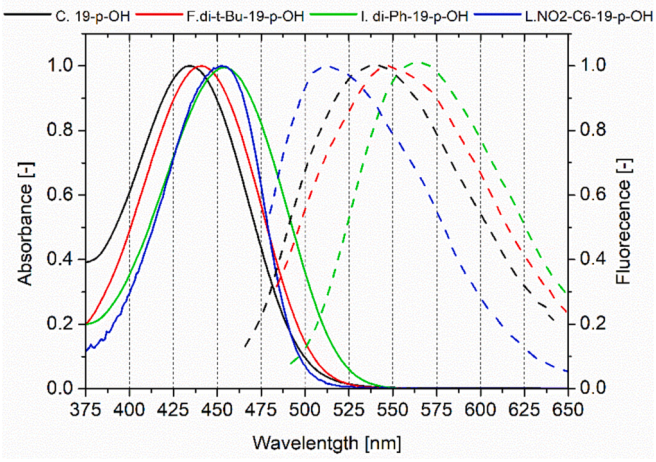

Fig. 3. Comparison of the absorption (solid) and emission (dashed) normalized spectra of 19-membered *p*-hydroxyazobenzocrowns **C**, **F**, **I**, **L** in acetonitrile.

The strength of the intramolecular hydrogen bond can be measured by the chemical shift value of the N–H proton signal. The stronger hydrogen bond the higher position [ppm] of the proton signal, which is engaged in the hydrogen bond formation. From the presented comparison it is clear that the strongest hydrogen bonded system occur for the smallest 13-membered macrocycles. In 16-membered crowns the position of signal of the N–H proton is found at lower ppm values indicating comparatively weaker hydrogen bond, when compared to 13-membered analogs. Furthermore, in 19-membered macrocycles with a longer oligoether chain, the increased flexibility of the molecule might contribute to a slight enhancement in the strength of the hydrogen bonds compared to the 16-membered p-hydroxyazobenzocrowns.

Another spectral measure of the strength of the hydrogen bond can be the position of the stretching vibrations band of N–H group in FTIR spectra. Therefore, the low-frequency shift of the vibrational band of the covalent N–H bond in infrared spectra of *p*-hydroxyazobenzocrowns was analyzed (ATR spectra, solid state). In Fig. 6 (left) FTIR spectra of unsubstituted macrocycles **A-C** are shown. Inset illustrates the position of the band of stretching vibrations of N–H group in compounds of different macrocycle size:13-, 16- and 19-membered. The strongest hydrogen bond system, estimated on the basis of the comparison of the position of νN-H band is for 13-membered crown **A**. The position of the N–H band shifts towards higher wavenumbers for 16-membered macrocycle pointing the weakening of the hydrogen bond. The difference between the position of the N–H vibration band for 16-membered (**B**) and 19-membered (**C**) crowns is not significant. Fig. 6 (right) presents the comparison of the position of the stretching vibrations band of N–H group in ATR spectra. Among series of macrocycles sharing identical substituents, but differing in size, the strongest hydrogen bonding is observed in the 13-membered macrocycles. Variations substituted macrocycles series could potentially arise due to steric and electron effects of substituents. However saying this, the trend of the position of the stretching vibrations band of the N–H group serving as a measure of the strength of the intramolecular bonding aligns with data obtained from ^{1}H NMR measurements in solution.

The analysis of the ^{1}H NMR and to some degree FTIR (solid state) data indicate that factors such as the size of the macrocycle and the stabilization of the quinone-hydrazone form via intramolecular hydrogen bond significantly influence the fluorescence properties, including the quantum yield values, of macrocycles **A-L**. This relationship is shown in Fig. 7 ilustrating the correlation between the position of the N–H proton signal in ^{1}H NMR spectra and quantum yields (QY).

The analysis of the quantum yields values (Fig. 4 and Fig. 7) shows that besides the macroring size, other factors, also influence at the fluorescence properties. The effect of substituents on the photoluminescence characteristics of different fluorophores, including tautomerizable azo derivatives, has been relatively widely studied in the literature [29,51–54]. Electron-donating groups in general increase the fluorescence. It is seen in case of macrocycles bearing two *tert*-butyl substituents, compounds **D-E**, (Fig. 4b, green frame), when comparing unsubstituted *p*-hydroxyazobenzocrowns **A-C**. Only in the case of the 13-membered compound **D**, it can be seen that the quantum yield is lower compared to the unsubstituted analog **A**. This may be due to the fact that two bulky substituents can significantly affect the structure of the molecule and reduce its planarity leading to reduced fluorescence. The highest values of quantum yield, among studied here macrocycles, have compounds **G-I** with two phenyl groups (Fig. 4b, orange frame). This could be attributed to the influence of phenyl groups on molecular geometry. The two extra aromatic rings increase the number of the conjugated double bonds which can also enhance the fluorescence [54].

The macrocycles **J-L** feature two additional functional groups: nitro group and *n*-hexyl moieties (Fig. 4b, violet frame) in opposite sides of molecule. The nitro group, as an electron-withdrawing substituent, is well known fluorescence quencher [54]. Nevertheless, there are known systems containing a nitro group that exhibit significant fluorescence properties [52,55]. The electro-donating effect of *n*-hexyl group is relatively small

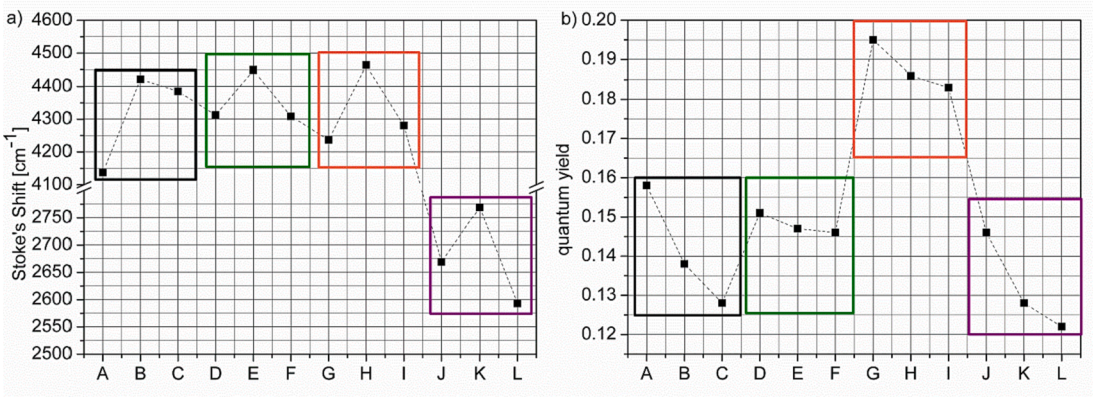

Fig. 4. The comparison of: a) Stoke's shift [cm^{-1}]; b) quantum yield values for compounds **A-L.**

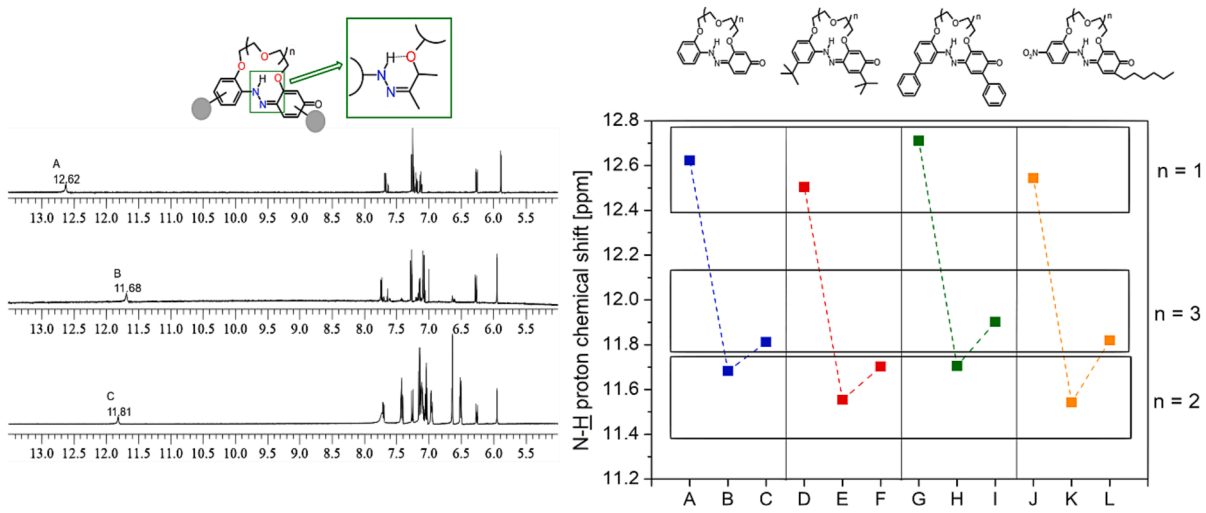

Fig. 5. Schematic representation of intramolecular hydrogen bond for *p*-hydroxyazobenzocrowns; partial ^{1}H NMR spectra of 13-, 16- and 19-membered macrocycles **A-C** (acetonitrile-d_3) and the position of the N–H proton signal in ^{1}H NMR spectra of macrocycles **A-L** in acetonitrile-d_3 (right).

[54] and additionally the long, alkyl chain can affect the molecular geometry, potentially reducing its planarity in comparison to the unsubstituted compounds. This can be a reason of the lowest fluorescence of this group of *p*-hydroxyazobenzocrowns. Another notable point of fluorescence properties of macrocycles **J-L** is their small Stoke's shift - the lowest among investigated series of *p*-hydroxyazobenzocrowns.

The azophenol ⇄ quinone-hydrazone tautomerism of macrocycles **A-L** was also investigated in theoretical studies. For all studied compounds, the structures (see: Table S1) were computed using the Gaussian [56]. In Fig. 8 the computed structures of macrocycles **A-C** in the quinone-hydrazone form are shown. The bottom line shows side views of molecules.

The calculated energy bandgaps for molecules **A-L** are compiled in Table 3 and presented in Fig. 9a.

The energy gap values plotted for molecules **A-L** (Fig. 9a) consistently indicate lower values for quinone-hydrazone tautomer compared to azophenol form. The results obtained by subtracting energies E_{tot}(AZ) and E_{tot}(QH) are positive in each case, pointing the higher stability of quinone-hydrazone form (Fig. 8b). This is in good agreement with the spectroscopic results obtained from solution and solid-state studies, namely FTIR studies and X-ray structure analysis of single crystals [37–39,57].

In Fig. 10 the relationship between certain experimental and theoretical data for compounds **A-L** are shown. The trends observed in the position of the emission maxima and Stokes's shift correlate with the energy gap E_g(QH) of quinone-hydrazone tautomer. The deviation from the observed trend is prominent for macrocycles **J**, **K** and **L** bearing nitro group, both in the position of emission band and the Stokes's shift.

When analyzing the computed energy parameters for both forms, a relationship can be observed: the smaller the difference in energies between the two forms, the lower the quantum yield. The lowest differences between the energies of both forms are characteristic for compounds containing a nitro group and a 6-membered alkyl chain, and these compounds have the lowest quantum yield. On the other hand, compounds containing two phenyl substituents exhibit the highest energy difference, matching with the highest observed quantum yield values. All above reflects the tendency of the *p*-hydroxyazobenzocrowns to exist in quinone-hydrazone form.

The characterization of fluorophores often involves assessing the dipole moment. Following molecular optimization, dipole moments were computed for both quinone-hydrazone and azophenol forms (Fig. 11a), and the obtained values are listed in Table S3. A trend observed in this comparison indicates that quinone-hydrazone tautomers generally exhibit higher polarity compared to their azophenol forms, which is well-documented in the literature [e.g., [58,59]]. However, it's important to note that compounds **J-L** characterize with higher dipole moment values for the azophenol tautomers, which aligns with expectations when considering these compounds as push–pull molecular systems.

Using solvatochromic method (vide experimental part and Supplementary Material) excited μ_e and ground μ_g state dipole moment values were estimated and compared (Fig. 11b) for compounds **A-L**. The values

Table 3
Spectroscopic properties and energy band gaps of molecules of compounds **A-L.**

Compound/ Substituents, macroring size	Chemical shift of N–H proton signal in ^{1}H NMR (acetonitrile) [ppm]*	Position of the vibrational band of N–H group (FTIR) [cm^{-1}]*	E_g(AZ) [eV]**	E_g(QH) [eV]**	E_{tot}(AZ) – E_{tot}(QH) [kJ/mol]
A. 13-*p*-OH	12.62	3260	3.62	3.15	45.35
B. 16-*p*-OH	11.68	3301	3.65	3.14	49.21
C. 19-*p*-OH	11.81	3307	3.58	3.11	45.35
D. di-*t*-Bu-13-*p*-OH	12.50	3261	3.59	3.10	46.21
E. di-*t*-Bu-16-*p*-OH	11.55	3315	3.61	3.09	53.30
F. di-*t*-Bu-19-*p*-OH	11.70	3324	3.55	3.07	46.31
G. di-Ph-13-*p*-OH	12.71	3261	3.49	2.97	50.17
H. di-Ph-16-*p*-OH	11.71	3301	3.51	2.97	52.10
I. di-Ph-19-*p*-OH	11.90	3325	3.46	2.94	50.17
J. NO2-C6-13-*p*-OH	12.54	3257	3.03	2.96	6.75
K. NO2-C6-16-*p*-OH	11.54	3305	3.08	2.97	10.61
L. NO2-C6-19-*p*-OH	11.82	3282	3.05	2.95	9.65

* Spectra are in Supporting Information.
** Calculated using Gaussian 16 [56]; AZ – azophenol and QH-quinone-hydrazone tautomers.

of excited and ground state dipole moment for macrocycles **A-L** are collected in Table S4. The calculations were performed for limited number of solvents (dichloromethane, acetonitrile, methanol and DMSO) so the data should be considered as approximate estimates. Nevertheless an interesting trend in the values of the excited state dipole moment can be observed. The value of the excited state dipole moment shows an increase corresponding to the increse of the macrocycle size in unsubstituted *p*-hydroxyazobenzocrowns **A-C**. Concerning macrocycles bearing substituents in benzene rings, the highest values of the excited state dipole moment were observed in the 16-membered crowns. Typically for fluorophores, the excited state dipole moment is higher than ground state dipole moment as it is observed for compounds **A-C** and **J-L**, and to smaller degree for **G** and **H**. For *t*-butyl derivatives **D-F** and 19-membered crown bearing two phenyl substituents (compound **I**) in ground state dipole moment is higher than in excited state. This may suggest that the distribution of charges in the excited state is more symmetrical or balanced compared to the ground state or be connected with the molecular geometry factors caused by the presence of bulky substituents and the flexibility of macroring in case of 19-membered crowns. The lower value of excited state dipole moment is not observed very often however it was reported for some cases. Namely for pyronin B [60] or ketones [61,62].

3. Conclusions

The spectroscopic properties of selected *p*-hydroxyazobenzocrowns were investigated. Among investigated macrocycles three compounds (**D**, **E** and **L**) are newly obtained. The analysis of the obtained quantum yields for compounds **A-L** indicates a dependency of fluorescence properties on macrocycle size: smaller macrorings exhibit higher

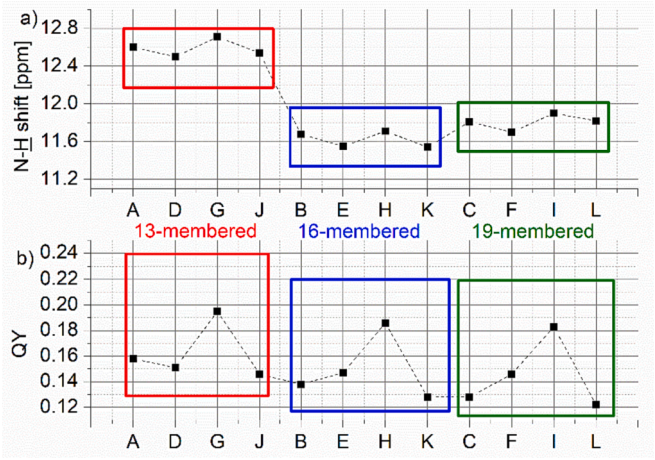

Fig. 7. A) the position of the N–H proton signal in ^{1}H NMR spectra of **A-L** (acetonitrile-d_3); b) quantum yields (QY) values for macrocycles **A-L** in acetonitrile.

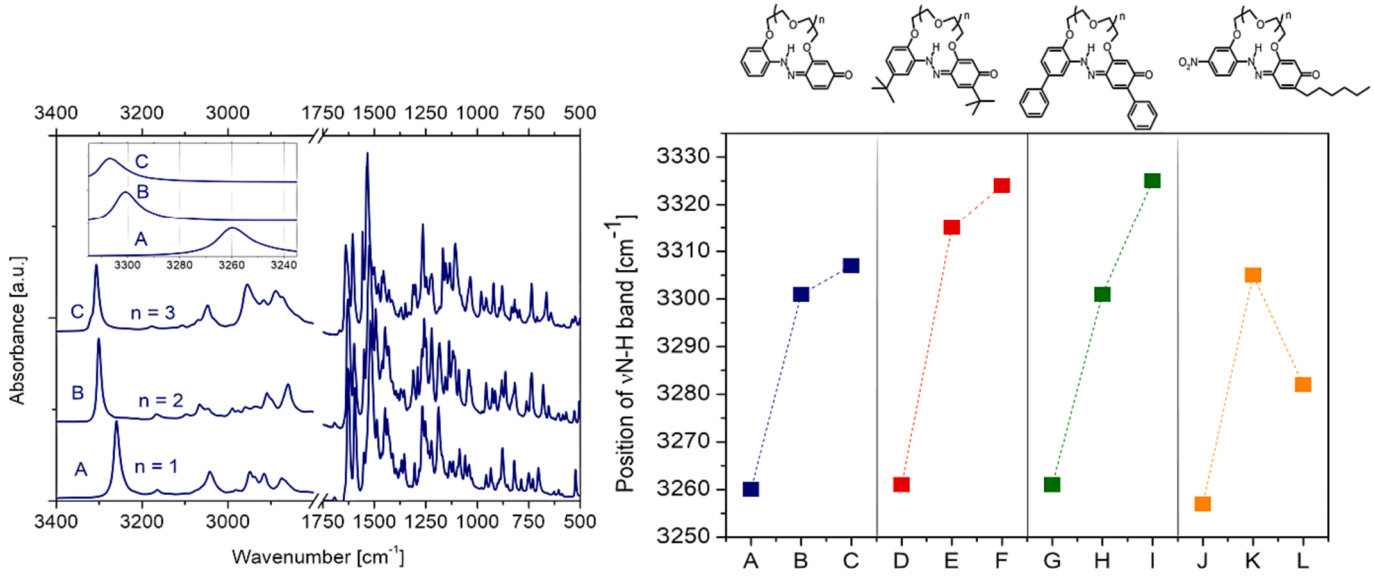

Fig. 6. FTIR spectra of 13-, 16- and 19-membered macrocycles **A-C** (left) and the position of the band of streching vibrations of N–H moiety in FTIR spectra of macrocycles **A-L** (right).

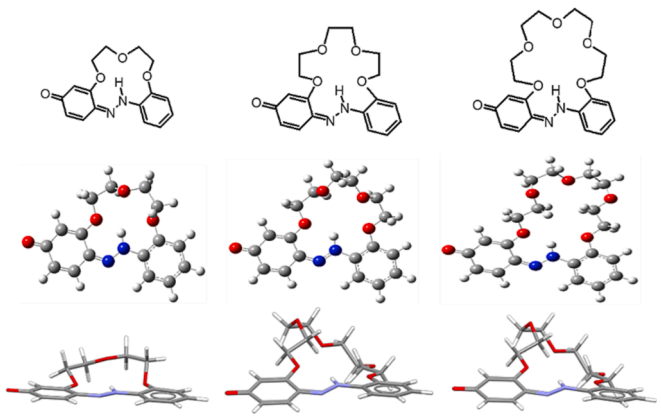

Fig. 8. Computed structures of quinone-hydrazone forms of molecules **A-C** (see: Theoretical studies).

quantum yield values. Compounds containing phenyl substituents show the highest value of quantum yield, which can be attributed to the presence of electron donating nature and geometrical effect of these substituents. Conversely compounds (**J-L**) with nitro group and a *n*-hexyl alkyl chain show the lowest quantum yield value and the smallest Stokes shift. Computed dipole moments for optimized structures confirmed higher polarity of push–pull macrocyles in their azophenol forms. Dipole moments of *p*-hydroxyazobenzocrowns in the ground and excited states have been determined. The polarity of macrocycles in the ground and excited states appears to depend on the size of the macrocycle and the presence of substituents in the benzene rings.

4. Experimental

4.1. Materials and methods

All used solvents and reagents were of analytical grade derived from Sigma-Aldrich or POCh. UV–Vis measurements were carried out with the use of an UNICAM UV 300 series spectrometer. Fluorescence spectra were recorded on a luminescence spectrometer (AMINCO Bowman Series 2 Spectrofluorimeter) with the flash xenon lamp. The bandpass of excitation and emission monochromators was 16 nm. UV–Vis and fluorescence measurements were carried out in 1 cm quartz cuvettes. UV–Vis absorption and emission spectra were normalized according to absorption/emission maximum. ^{1}H and ^{13}C NMR spectra were recorded on a Varian INOVA 500 spectrometer at 500 and at 125 MHz,

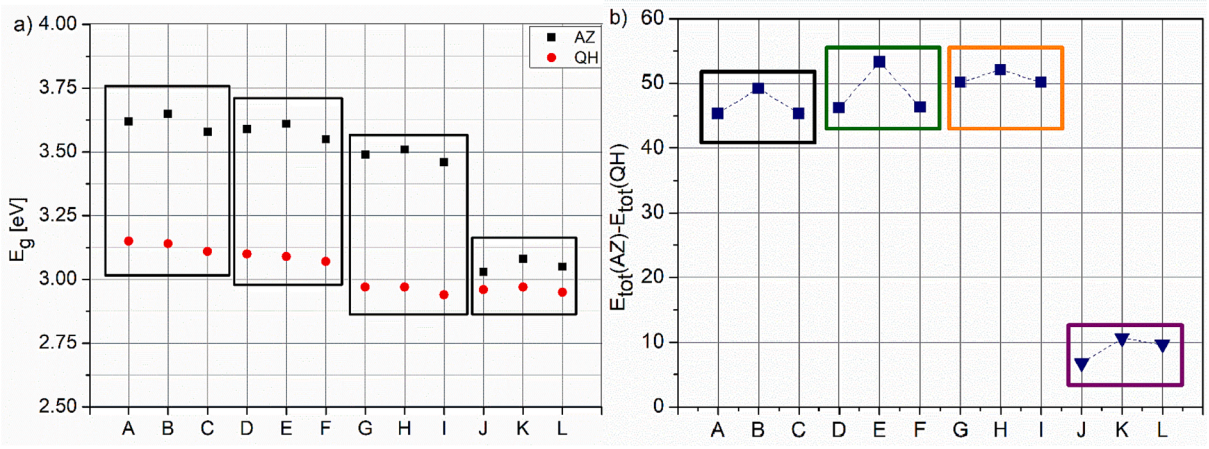

Fig. 9. A) plot of energy gap values of compounds **A-L** calculated using DFT-B3LYP/6-31+G (AZ - azophenol, QH - quinone-hydrazone forms of **A-L**); b) the difference between the energies of azophenol and quinone-hydrazone tautomers of compounds **A-L**.

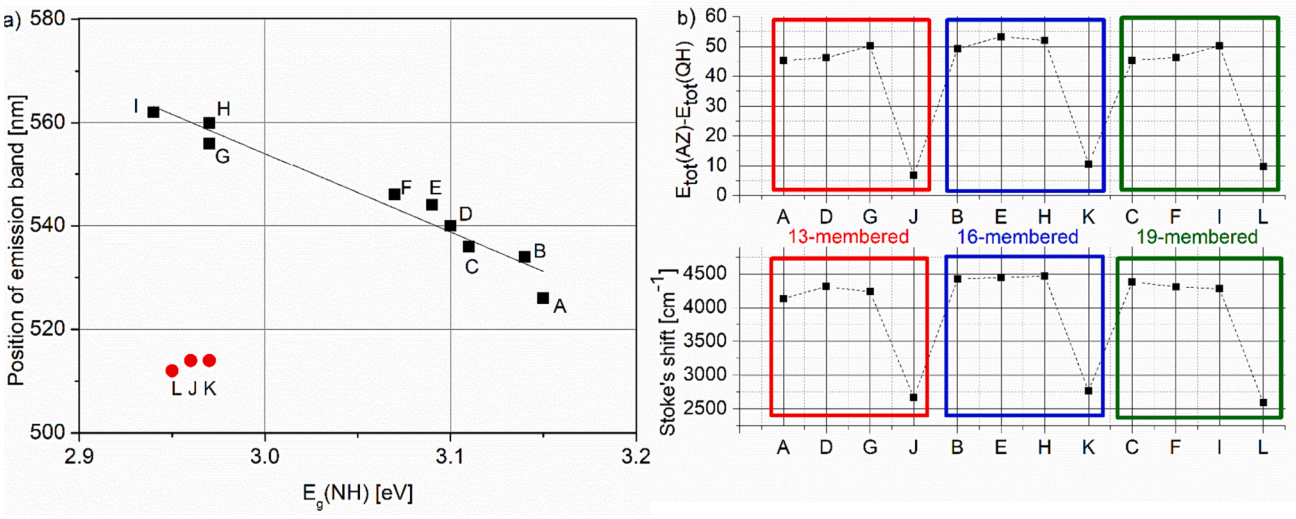

Fig. 10. a) Energy band gaps for quinone-hydrazone (QH) form of compounds **A-L** vs. position of fluorescence maximum in acetonitrile; b) the comparison of the energy band gaps with the Stoke's shift values for macrocycles **A-L**.

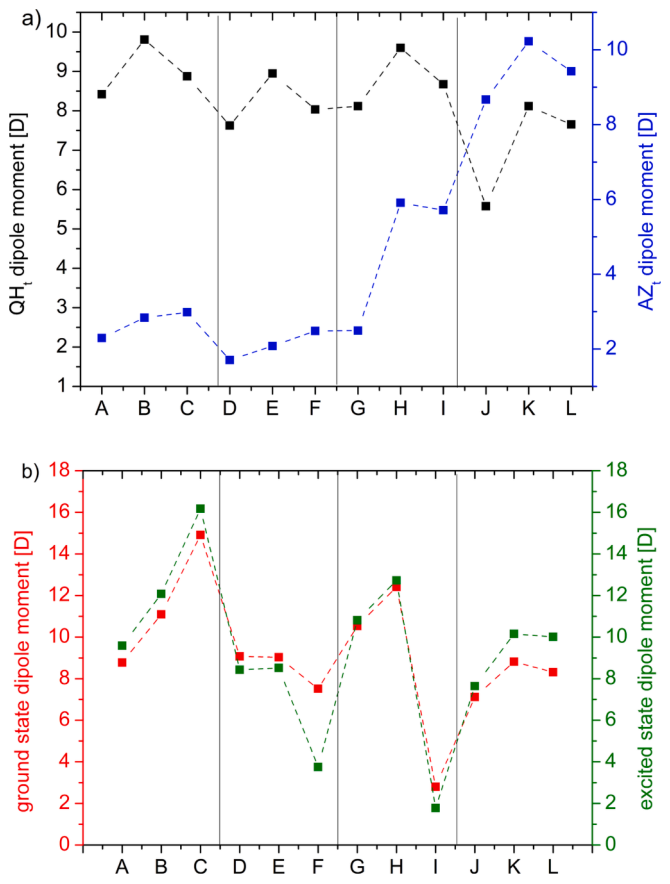

Fig. 11. A) dipole moments calculated for optimized structures of molecules **A-L**; b) calculated (experimental spectroscopic data) values of ground and excited state dipole moments for molecules **A-L**.

respectively. Chemical shifts are reported in δ (ppm) units. FTIR spectra (film or ATR) were taken on Nicolet iS10 apparatus. All ATR FTIR spectra were ATR and baseline corrected using spectrophotometer commercial software. Spectra were normalized according to signal of the highest intensity. High resolution mass spectra (HRMS) were taken on a SYNAPT G2-S HDMS (Waters) spectrometer with electrospray ionization source (ESI) and a TOF mass analyzer. Photochemical reactions were carried out in quartz flasks using a photoreactor prototype designed by Dariusz Wysiecki MSc. Eng. and constructed in cooperation with the Enviklim Company (Gdańsk, Poland). The reactor is equipped with 3 UVA diode arrays (2xUV-D6565-4LED, 40 W and 1xUV-D6565-15LED, 150 W, λ = 365–370 nm).

The reaction progress and purity of products were monitored by TLC using aluminum sheets covered with silica gel 60F$_{254}$ (Merck). UV light (254 nm) was used as the detection method. Reaction mixtures were separated using a classical column (silica gel 60, 0.063–0.200 mm, Merck) or preparative thin layer chromatography (PLC plates, silica gel 60F$_{254}$, 1 mm, 20 × 20 cm size, Merck). Reagent grade solvents were used.

4.2. Determination of quantum yield

Quantum yield standard. The standard for determining the quantum yield was selected so that it absorbs and emits in a similar wavelength range as the studied compound. Therefore, fluorescein (λ_{ex} = 490 nm, λ_{em} = 520 nm, 0.1 M NaOH as solvent) was chosen as a standard for the study of compounds **A-L**.

Determination of the fluorescence quantum yield of hydroxyazobenzocrown consisted of the following steps: (i) registration of absorption spectra of the particular hydroxyazobenzocrown and standard solutions in concentration of absorbance below 0.1, (ii) selection of standard so that the measurement range of the standards would match that of the sample (iii) registration of the emission spectra of hydroxyazobenzocrown and standard solution (instrument settings, excitation wavelength λ_{ex} and emission wavelength λ_{em} the same for the standard and sample: λ_{ex} = 434 nm, λ_{em} = 536 nm), (iiii) calculation of quantum yield using equation (1), where x - sample, s - standard, QY - quantum yield, a - slope of the plot line A = f(F), where: F – integrated intensities of spectra, area under the emission spectrum, A - absorbance value at maximum of absorption [63–67].

$$QY_x = \frac{a_x}{a_s} \bullet QY_s \tag{1}$$

4.3. Determination of the dipole moment in ground and excited states

The excited μ_e and ground μ_g state dipole moments were estimated using solvatochromic method [68–71]. The calculations were based on difference (2) and sum (3) in absorption ν_a and emission ν_f [cm^{-1}] band shifts and the solvent polarity functions (2a, 3a):

$$\nu_a - \nu_f = m_1 f(\varepsilon_r, n) + const \tag{2}$$

where n stands for refractive index of the solvent, ε_r is permittivity of the solvent

$$f(\varepsilon_r, n) = \frac{2n^2+1}{n^2+2}\left(\frac{\varepsilon_r - 1}{\varepsilon_r + 2} - \frac{n^2-1}{n^2+2}\right) \tag{2a}$$

$$\nu_a + \nu_f = -m_2[f(\varepsilon_r, n) + 2\ g(n)] + const \tag{3}$$

and solvent polarity function (3a):

$$g(n) = \frac{3}{2}\left(\frac{n^4-1}{(n^2+2)^2}\right) \tag{3a}$$

Plots $\nu_a - \nu_f$ vs. $f(\varepsilon_r, n)$ and $\nu_a + \nu_f$ vs. $[f(\varepsilon,n) + 2\ g(n)]$ allow to obtain m_1 and m_2 parameters:

$$m_1 = \frac{2(\mu_e - \mu_g)^2}{hca^3} \tag{4}$$

$$m_2 = \frac{2(\mu_e^2 - \mu_g^2)}{hca^3} \tag{5}$$

where h – Planck's constant, c is the velocity of the light in vacuum, μ_e and μ_g are the excited and ground state dipole moments, a – is Onsager cavity radius.

Onsager cavity radius was calculated according to equation (6) [71]:

$$V_{vdW} = \frac{4}{3}\pi a^3 \tag{6}$$

where V_{vdW} is van der Waals volume (Å^3/molecule) and can be calculated using formula (7) below:

$$V_{vdW} = \sum(allatomcontributions) - 5.92N_B - 14.7R_A - 3.8R_{NA} \tag{7}$$

N_B is the number of bonds, R_A is the number of aromatic rings, and R_{NA} is the number of non-aromatic rings. If the total number of atoms in the molecule is N, then the number of bonds N_B can be calculated using formula (8):

$$N_B = N - 1 + R_A + R_{NA} \tag{8}$$

The van der Waals volumes (V_{vdW}) for carbon, hydrogen, nitrogen and oxygen are: 20.58, 7.24, 1.55 and 14.71 Å^3 [72], respectively.1 For example, the molecular formula of **A** is C16H16N2O4. Thus, the sum of all atom contribution for this molecule can be calculated as:

$$\sum(allatomcontributions) = (16 \times 20.58) + (16 \times 7.24) + (2 \times 1.55) + (4 \times 14.71) = 535.16$$

Calculated values of van der Waals volume and Onsager cavity radii are listed in Table S2.

On the basis of above the dipole moments of compounds **A**-**L** in the ground (μ_g) and excited (μ_e) were estimated according to equations:

$$\mu_g = \frac{|m_2 - m_1|}{2}\left(\frac{hca^3}{2m_1}\right)^{\frac{1}{2}} \quad (9)$$

$$\mu_e = \frac{|m_1 + m_2|}{|m_2 - m_1|}\left(\frac{hca^3}{2m_1}\right)^{\frac{1}{2}} \quad (10)$$

Note: Dipole moment values in the Lippert-Mataga equation is in the unit of esu cm. Conversion of units: 1D = 1×10^{-18} esu cm, 1 esu = 1 $g^{1/2}$ $cm^{3/2}$ s^{-1}, 1 erg = g cm^2 s^{-2}; Planck constant, h = 6.626×10^{-27} erg s; speed of light, c = 3×10^{10} cm s^{-1}; 1 Å = 1×10^{-8}cm.

The values of obtained dipole moments determined on the basis of the spectral measurements in acetonitrile, DMSO, methanol and dichloromethane are listed in Table S3.

4.4. Theoretical studies

Starting conformations of the molecules were based on structures of similar compounds deposited to CSD [73]. For each compound, quinone-hydrazone and azophenol isomers were prepared. Then the optimizations were performed *in vacuo* using Gaussian 16 [56] at B3LYP/6–31+G(d,p) level of theory with Grimme's D3 dispersion correction. In each case the vibrational analysis showed that there are no negative frequencies, so the optimized structures are in a local minimum of the potential energy surface. Bandgaps were calculated as a simple HOMO-LUMO energy differences. Dipole moments have been calculated for molecules after optimization.

CRediT authorship contribution statement

Paulina Szulc: Conceptualization, Data curation, Investigation, Methodology, Validation, Visualization, Writing – original draft, Writing – review & editing. **Elżbieta Luboch:** Conceptualization, Investigation, Methodology, Writing – review & editing. **Andrzej Okuniewski:** Data curation, Formal analysis, Investigation, Methodology, Writing – original draft. **Ewa Wagner-Wysiecka:** Conceptualization, Supervision, Visualization, Formal analysis, Investigation, Writing – original draft, Writing – review & editing. All authors discussed the results and commented on the manuscript.

Declaration of competing interest

The authors declare that they have no known competing financial interests or personal relationships that could have appeared to influence the work reported in this paper.

Data availability

Data will be made available on request.

Acknowledgments

This work was supported by the Faculty of Chemistry, Gdańsk University of Technology, No. 036277 - an internal grant from statutory funds. The financial support to maintenance of research facilities used in these studies from Gdańsk University of Technology by the DEC-2/2021/IDUB/V.6/Si grant under the SILICIUM SUPPORTING CORE R&D FACILITIES – "Excellence Initiative - Research University" program is gratefully acknowledged. Joanna Woszczyk, Dr. Paweł Sowiński, Dr. Katarzyna Szwarc-Karabyka (Gdańsk University of Technology, Faculty of Chemistry, Nuclear Magnetic Resonance Laboratory) are kindly acknowledged for spectra registration.

Appendix A. Supplementary material

Supplementary data to this article can be found online at https://doi.org/10.1016/j.saa.2023.123721.

References

[1] F.A. Jerca, V.V. Jerca, R. Hoogenboom, Advances and opportunities in the exciting world of azobenzenes, Nat. Rev. Chem. 6 (2022) 51–69, https://doi.org/10.1038/s41570-021-00334-w.
[2] E. Wagner-Wysiecka, N. Łukasik, J.F. Biernat, E. Luboch, Azo group(s) in selected macrocyclic compounds, J. Incl. Phenom. Macrocycl. Chem. 90 (2018) 189–257, https://doi.org/10.1007/s10847-017-0779-4.
[3] M. Shiga, H. Nakamura, M. Takagi, K. Ueno, Synthesis of azobenzocrown ethers and their complexation behavior with metal ions, Bull. Chem. Soc. Jpn. 57 (1984) 412–415, https://doi.org/10.1246/bcsj.57.412.
[4] R. Tahara, T. Morozumi, H. Nakamura, M. Shimomura, Photoisomerization of azobenzocrown ethers. Effect of complexation of alkaline earth metal ions, J. Phys. Chem. B. 101 (1997) 7736–7743, https://doi.org/10.1021/jp9701000.
[5] J.F. Biernat, E. Luboch, A. Cygan, New macrocycles containing the azoxy subunit and their properties, J. Coord. Chem. 27 (1992) 215–217, https://doi.org/10.1080/00958979209407953.
[6] E. Wagner-Wysiecka, M. Szarmach, J. Chojnacki, N. Łukasik, E. Luboch, Cation sensing by diphenyl-azobenzocrowns, J. Photochem. Photobiol. Chem. A 333 (2017) 220–232, https://doi.org/10.1016/j.jphotochem.2016.10.028.
[7] M. Szarmach, E. Wagner-Wysiecka, M.S. Fonari, E. Luboch, Bis(azobenzocrown ether)s - synthesis and ionophoric properties, Tetrahedron 68 (2012) 507–515, https://doi.org/10.1007/s10847-017-0779-4.
[8] E. Luboch, E. Wagner-Wysiecka, J.F. Biernat, Chromogenic azocrown ethers with peripheral alkyl, alkoxy, hydroxy or dimethylamino group, Supramol. Chem. 2 (2002) 279–291, https://doi.org/10.1007/s10847-017-0779-4.
[9] E. Luboch, J.F. Biernat, Y.A. Simonov, V.C. Kravtsov, V.K. Bel'skii, Structures of NaI complexes of 16-membered azo- and azoxycrown ethers. Correlation of crystal structure and carrier-doped membrane electrode selectivity, Supramol. Chem. 11 (1999) 109–118, https://doi.org/10.1080/10610279908048722.
[10] E. Luboch, J.F. Biernat, Y.A. Simonov, A.A. Dvorkin, Synthesis and electrode properties of 16-membered azo- and azoxycrown ethers. Structure of tribenzo-16-azocrown-6, Tetrahedron 54 (1998) 4977–4990, https://doi.org/10.1016/S0040-4020(98)00203-8.
[11] E. Luboch, J.F. Biernat, E. Muszalska, R. Bilewicz, 13-Membered crown ethers with azo or azoxy unit in the macrocycle - synthesis, membrane electrodes, voltammetry and Langmuir monolayers, Supramol. Chem. 5 (1995) 201–210, https://doi.org/10.1080/10610279508028948.
[12] E. Luboch, E. Wagner-Wysiecka, Z. Poleska-Muchlado, V.C. Kravtsov, Synthesis and properties of azobenzocrown ethers with π-electron donor, or π-electron donor and π-electron acceptor group(s) on benzene ring(s), Tetrahedron 61 (2005) 10738–10747, https://doi.org/10.1016/j.tet.2005.08.071.
[13] E. Luboch, E. Wagner-Wysiecka, T. Rzymowski, 4-Hexylresorcinol-derived hydroxyazobenzocrown ethers as chromoionophores, Tetrahedron 65 (2009) 10671–10678, https://doi.org/10.1016/j.tet.2009.10.054.
[14] H. Rau, Spectroscopic properties of organic azo compounds, Angew. Chem. Int. Ed. 12 (1973) 224–235, https://doi.org/10.1002/anie.197302241.
[15] H. Bisle, H. Rau, Fluorescence of noncyclic azo compounds with a low-lying 1(n, π*) state, Chem. Phys. Lett. 31 (1975) 264–266, https://doi.org/10.1016/0009-2614(75)85017-2.
[16] H. Rau, Radiative and radiationless radiative and radiationless decay of excited state of azo compounds, J. Lumin. 1–2 (1970) 191–199, https://doi.org/10.1016/0022-2313(70)90034-7.
[17] P.S. Zacharias, S. Ameerunisha, S.R. Korupoju, Photoinduced fluorescence changes on E-Z isomerisation in azobenzene derivatives, J. Chem. Soc. Perkin Trans. 2 (1998) 2055–2059, https://doi.org/10.1039/A706775E.
[18] E. Wagner-Wysiecka, T. Rzymowski, M. Szarmach, M.S. Fonari, E. Luboch, Functionalized azobenzocrown ethers as sensor materials—The synthesis and ion binding properties, Sens. Actuators B: Chem. 177 (2013) 913–923, https://doi.org/10.1016/j.snb.2012.11.068.
[19] G. Gabor, E. Fischer, Tautomerism and geometrical isomerism in arylazophenols and naphtols. Part II. 2-Phenyloazo-3-naphtol. The effect of internal hydrogen bonds on photoisomerization. Part I, J. Phys. Chem. 66 (1962) 2478–2481, https://doi.org/10.1021/j100818a037.
[20] G. Gabor, Y. Frei, D. Gegiou, M. Kaganowitch, E. Fischer, Tautomerism and geometric isomerism in arylazo-phenols and naphthols. Part III. Orthohydroxy derivatives and their reversible photochemical reactions, Isr. J. Chem. 5 (1967) 193–212, https://doi.org/10.1002/ijch.196700037.
[21] G. Gabor, Y. Frei, E. Fischer, Tautomerism and geometric isomerism in arylazophenols and naphthols. IV. Spectra and reversible photoreactions of m- and p-hydroxyazobenzene, J. Phys. Chem. 72 (1968) 3266–3272, https://doi.org/10.1021/J100855A029.

[22] H. Rau, Über die fluoreszenz der hydroxyazoverbindungen, Bunsenges. Phys. Chem. 72 (1969) 637–643, https://doi.org/10.1002/bbpc.19680720508.

[23] D. Gegiou, E. Fischer, The emission properties of ortho-phenylazo-phenols and naphthols, Chem. Phys. Lett. 10 (1971) 99–101, https://doi.org/10.1016/0009-2614(71)80434-7.

[24] S.J. Porobić, B.D. Božić, M.D. Dramićanin, V. Vitnik, Ž. Vitnik, M. Marinović-Cinović, D.Ž. Mijin, Absorption and fluorescence spectral properties of azo dyes based on 3-amido-6-hydroxy-4-methyl-2-pyridone: Solvent and substituent effects, Dyes Pigm. 175 (2020), 108139, https://doi.org/10.1016/j.dyepig.2019.108139.

[25] M. Simomura, T. Kunitake, Fluorescence and photoisomerization of azobenzene-containing bilayer membranes, J. Am. Chem. Soc. 109 (1987) 5175–5183, https://doi.org/10.1021/ja00251a022.

[26] B. Bisht, P. Bhardwaj, M. Giri, S. Pant, Fluorescence spectral properties of methyl orange in homogeneous media, J. Fluoresc. 31 (2021) 1787–1795, https://doi.org/10.1007/s10895-021-02820-2.

[27] B. Bisht, S. Pant, M. Giri, Static and dynamic fluorescence spectroscopic analyses of direct yellow 27—an azo dye, Indian J. Phys. 96 (2022) 895–901, https://doi.org/10.1007/s12648-021-02040-1.

[28] H. Puchtler, F. Sweat, S. Gropp, An investigation into the relation between structure and fluorescence of azo dyes, J. Microsc. 87 (1967) 309–328, https://doi.org/10.1111/j.1365-2818.1967.tb04513.x.

[29] J. Yoshino, A. Furuta, T. Kambe, H. Itoi, N. Kano, T. Kawashima, Y. Ito, M. Asashima, Intensely fluorescent azobenzenes: synthesis, crystal structures, effects of substituents, and application to fluorescent vital stain, Chem. Eur. J. 16 (2010) 5026–5035, https://doi.org/10.1002/chem.201000258.

[30] E. Hosgor, A. Akdag, Synthesis of azobenzene - containing macrocycles exhibiting unexpected fluorescence, Chem. Pap. 76 (2022) 3891–3898, https://doi.org/10.1007/s11696-022-02133-z.

[31] S. Mabhai, M. Dolai, S.K. Dey, S.M. Choudhury, B. Das, S. Dey, A. Jana, D. R. Banerjee, A naphthalene-based azo armed molecular framework for selective sensing of Al^{3+}, New. J. Chem. 46 (2022) 6885–6898, https://doi.org/10.1039/D1NJ05869J.

[32] Z. Badr, M.A. Abdel-Lateef, H. Gomaa, M. Abdelmottaleb, M. Taher, Spectrofluorimetric determination of magnesium ions in water, ampoule, and suspension samples using a fluorescent azothiazol-benzenesulfonamide derivative, Luminescence 37 (2022) 448–454, https://doi.org/10.1002/bio.4193.

[33] A. Chevalier, P.Y. Renard, A. Romieu, Azo-based fluorogenic probes for biosensing and bioimaging: recent advances and upcoming challenges, Chem. Asian J. 12 (2017) 2008–2028, https://doi.org/10.1002/asia.201700682.

[34] L. Xue, Y. Pan, S. Zhang, Y. Chen, H. Yu, Y. Yang, L. Mo, Z. Sun, L. Li, H. Yang, Fluorescent azobenzene-containing compounds: from structure to mechanism, Crystals 11 (2021) 840, https://doi.org/10.3390/cryst11070840.

[35] M. Homocianu, A. Airinei, D.O. Dorohoi, Solvent effects on the electronic absorption and fluorescence spectra, J. Adv. Res. Phys. 2 (2011), 011105.

[36] M. Szarmach, E. Wagner-Wysiecka, E. Luboch, Rearrangement of azoxybenzocrowns into chromophoric hydroxyazobenzocrowns and the use of hydroxyazobenzocrowns for the synthesis of ionophoric biscrown compounds, Tetrahedron 69 (2013) 10893–10905, https://doi.org/10.1016/j.tet.2013.10.074.

[37] E. Wagner-Wysiecka, P. Szulc, E. Luboch, J. Chojnacki, K. Szwarc-Karabyka, N. Łukasik, M. Murawski, M. Kosno, Photochemical rearrangement of a 19-membered azoxybenzocrown: products and their properties, ChemPlusChem 85 (2020) 2067–2083, https://doi.org/10.1002/cplu.202000474.

[38] E. Wagner-Wysiecka, P. Szulc, E. Luboch, J. Chojnacki, P. Sowiński, K. Szwarc-Karabyka, Products of photo- and thermochemical rearrangement of 19-membered di-*tert*-butyl-azoxybenzocrown, Molecules 27 (2022) 1835, https://doi.org/10.3390/molecules27061835.

[39] E. Wagner-Wysiecka, P. Szulc, E. Luboch, J. Chojnacki, D. Laskowska, P. Miklaszewska, P. Sowiński, Do Phenyl substituents affect the properties of azobenzocrown derivatives? ChemPlusChem. 88 (2023) e202300175, https://doi.org/10.1002/cplu.202300175.

[40] J. Premakumari, G.A.G. Roy, A.A.M. Prabhu, G. Venkatesh, V.K. Subramanian, N. Rajendiran, Effect of solvents and pH on β-cyclodextrin inclusion of 2,4-dihydroxyazobenzene and 4-hydroxyazobenzene, J. Solution Chem. 40 (2011) 327–347, https://doi.org/10.1007/s10953-010-9639-1.

[41] J. Griffiths, Prediction of colour change in dye equilibria I-azo and hydrazone tautomers and anions of 4-phenylazo-1-naphthols, J. Soc. Dye. Colour. 88 (1972) 106–109, https://doi.org/10.1111/j.1478-4408.1972.tb03066.x, practical and theoretical aspect.

[42] L. Baldini, D. Balestri, L. Marchiò, A. Casnati, A combined solution and solid-state study on the tautomerism of an azocalix[4]arene chromoionophore, Molecules 28 (2023) 4704–4716, https://doi.org/10.3390/molecules28124704.

[43] G.S. Ušćumlić, D.Z. Mijin, N.V. Valentić, V.V. Vajs, B.M. Sušić, Substituent and solvent effects on the UV/Vis absorption spectra of 5-(4-substituted arylazo)-6-hydroxy-4-methyl-3-cyano-2-pyridones, Chem. Phys. Lett. 397 (2004) 148–153, https://doi.org/10.1016/j.cplett.2004.07.057.

[44] M.R. Yazdanbakhsh, M. Giahi, A. Mohammadi, Synthesis and solvatochromic properties of some new disperse azo dyes derived from 2-anilinoethanol, J. Mol. Liq. 144 (2009) 145–148, https://doi.org/10.1016/j.molliq.2008.10.013.

[45] A. Mohammadi, M.R. Yazdanbakhsh, L. Farahnak, Synthesis and evaluation of changes induced by solvent and substituent in electronic absorption spectra of some azo disperse dyes, Spectroc. Acta Part A. 89 (2012) 238–242, https://doi.org/10.1016/j.saa.2011.12.062.

[46] C.D. Gabbutt, B. Mark Heron, A.C. Instone, The synthesis and electronic absorption spectra of 3-phenyl-3(4-pyrrolidino-2-substituted phenyl)-3H-naphtho[2,1-b] pyrans: further exploration of the ortho substituent effect, Tetrahedron 62 (2006) 737–745, https://doi.org/10.1016/j.tet.2005.09.143.

[47] H. Joshi, F.S. Kamounah, C. Gooijer, G. van der Zwan, L. Antonov, Excited state intramolecular proton transfer in some tautomeric azo dyes and Schiff bases containing an intramolecular hydrogen bond, J. Photochem. Photobiol. A Chem. 152 (2002) 183–191, https://doi.org/10.1016/S1010-6030(02)00155-7.

[48] M. Dračínský, The chemical bond: The perspective of NMR spectroscopy, Ann. Rep. NMR Spectrosc. 90 (2016) 1–40, https://doi.org/10.1016/bs.arnmr.2016.07.001.

[49] M.G. Siskos, M.I. Choudhary, I.P. Gerothanassis, Hydrogen atomic positions of O-H···O hydrogen bonds in solution and in the solid state: the synergy of quantum chemical calculations with 1H-NMR chemical shifts and X-ray diffraction methods, Molecules 22 (2017) 415, https://doi.org/10.3390/molecules22030415.

[50] A.V. Afonin, I.V. Sterkhova, A.V. Vashchenko, M.V. Sigalov, Estimating the energy of intramolecular bifurcated (three-centered) hydrogen bond by X-ray, IR and 1H NMR spectroscopy, and QTAIM calculations, J. Mol. Str. 1163 (2018) 185–196, https://doi.org/10.1016/j.molstruc.2018.02.106.

[51] T. Aysha, S. Luňák Jr., Lyčka, R. Hrdina, Synthesis, absorption and fluorescence of hydrazone colorants based on pyrrolinone esters, Dyes Pigm. 91 (2011) 170–176, https://doi.org/10.1016/j.dyepig.2011.03.013.

[52] H.M. Alsoghier, M. Abdellah, H.M. Rageh, H.M.A. Salman, M.A. Selim, M. A. Santos, S.A. Ibrahim, NMR spectroscopic investigation of benzothiazolylacetonitrile azo dyes: CR7 substitution effect and semiempirical study, Results Chem. 3 (2021), 100088, https://doi.org/10.1016/j.rechem.2020.100088.

[53] S.A. Elroby, K.H. Aloufi, S.G. Aziz, A. Jedidi, W.I. Hassan, O.I. Osman, Substituent effect on the intramolecular hydrogen bond and the proton transfer process in pyrimidine azo dye : A computational study, Results Chem. 6 (2023), 101034, https://doi.org/10.1016/j.rechem.2023.101034.

[54] R.T. Williams, J.W. Bridges, Fluorescence of solutions: A review, J. Clin. Pathol. 17 (1964) 371–394, https://doi.org/10.1136/jcp.17.4.371.

[55] M.C. Chen, D.G. Chen, P.T. Chou, Fluorescent chromophores containing the nitro group: relatively unexplored emissive properties, ChemPlusChem. 86 (2021) 11–27, https://doi.org/10.1002/cplu.202000592.

[56] M.J. Frisch, G.W. Trucks, H.B. Schlegel, G.E. Scuseria, M.A. Robb, J.R. Cheeseman, G. Scalmani, V. Barone, G.A. Petersson, H. Nakatsuji, X. Li, M. Caricato, A. V. Marenich, J. Bloino, B.G. Janesko, R. Gomperts, B. Mennucci, H.P. Hratchian, J. V. Ortiz, A.F. Izmaylov, J.L. Sonnenberg, D. Williams-Young, F. Ding, F. Lipparini, F. Egidi, J. Goings, B. Peng, A. Petrone, T. Henderson, D. Ranasinghe, V. G. Zakrzewski, J. Gao, N. Rega, G. Zheng, W. Liang, M. Hada, M. Ehara, K. Toyota, R. Fukuda, J. Hasegawa, M. Ishida, T. Nakajima, Y. Honda, O. Kitao, H. Nakai, T. Vreven, K. Throssell, J.A. Montgomery Jr., J.E. Peralta, F. Ogliaro, M. J. Bearpark, J.J. Heyd, E.N. Brothers, K.N. Kudin, V.N. Staroverov, T.A. Keith, R. Kobayashi, J. Normand, K. Raghavachari, A.P. Rendell, J.C. Burant, S.S. Iyengar, J. Tomasi, M. Cossi, J.M. Millam, M. Klene, C. Adamo, R. Cammi, J.W. Ochterski, R.L. Martin, K. Morokuma, O. Farkas, J.B. Foresman, D.J. Fox, Gaussian 16, Revision C.01, Gaussian Inc, Wallingford CT, 2016.

[57] E. Luboch, V.C. Kravtsov, Molecular structures and supramolecular architectures of two chromogenic 13-membered azobenzocrown ethers with a peripheral hydroxyl group in the benzene ring, J. Mol. Struct. 699 (2004) 9–15, https://doi.org/10.1016/j.molstruc.2003.12.026.

[58] A. Antony Muthu Prabhu, G. Venkatesh, N. Rajendiran, Azo-hydrazo tautomerism and inclusion complexation of 1-phenylazo-2-naphthols with various solvents and β-cyclodextrin, J. Fluoresc. 20 (2010) 961–972, https://doi.org/10.1007/s10895-010-0642-0.

[59] D. Zheng, Y. Gu, X. Li, L. Zhang, W. Zhao, J. Ma, Hydrogen bonding promoted tautomerism between azo and hydrazone forms in calcon with multistimuli responsiveness and biocompatibility, J. Chem. Inf. Model. 59 (2019) 2110–2122, https://doi.org/10.1021/acs.jcim.8b00985].

[60] B. Acemioğlua, Y. Onganerb, Determination of ground- and excited-state dipole moments of pyronin B using the solvatochromic method and quantum-chemical calculations, Acta Phys. Pol. A 138 (2020) 546–553, https://doi.org/10.12693/APhysPolA.138.546.

[61] M. Ito, K. Inuzuka, S. Imanish, Effect of solvent on n-π* absorption spectra of ketones, J. Am. Chem. Soc. 82 (1960) 1317–1322, https://doi.org/10.1021/ja01491a011.

[62] T. Abe, The dipole moment and polarizability in the n-π* excited state of acetone from spectral solvent shifts, Bull. Chem. Soc. Jpn. 39 (1966) 936–939, https://doi.org/10.1246/bcsj.39.936.

[63] J.H. Brannon, D. Madge, Absolute quantum yield determination by thermal blooming. fluorescein, J. Phys. Chem. 82 (1978) 705–709, https://doi.org/10.1021/j100495a018.

[64] A.M. Brouwer, Standards for photoluminescence quantum yield measurements in solution (IUPAC Technical Report), Pure Appl. Chem. 83 (2011) 2213–2228, https://doi.org/10.1351/PAC-REP-10-09-31.

[65] C.L. Renschler, L.A. Harrah, Determination of quantum yields of fluorescence by optimizing the fluorescence intensity, Anal. Chem. 55 (1983) 798–800, https://doi.org/10.1021/ac00255a050.

[66] H. Ishida, J.-C. Bünzli, A. Beeby, Guidelines for measurement of luminescence spectra and quantum yields of inorganic and organometallic compounds in solution and solid state (IUPAC Technical Report), Pure Appl. Chem. 88 (2016) 701–711, https://doi.org/10.1515/pac-2014-0706.

[67] R.A. Velapoldi, H.H. Tønnesen, Corrected emission spectra and quantum yields for a series of fluorescent compounds in the visible spectral region, J. Fluoresc. 14 (2004) 465–472, https://doi.org/10.1023/B:JOFL.0000031828.96368.c1.

[68] A. Belay, E. Libnedengel, H.K. Kim, Y.-H. Hwang, Effects of solvent polarity on the absorption and fluorescence spectra of chlorogenic acid and caffeic acid compounds: determination of the dipole moments, Luminescence. 31 (2016) 118–126, https://doi.org/10.1002/bio.2932.

[69] U.S. Raikar, C.G. Renuka, Y.F. Nadaf, B.G. Mulimani, A.M. Karguppikar, M. K. Soudagar, Solvent effects on the absorption and fluorescence spectra of coumarins 6 and 7 molecules: Determination of ground and excited state dipole moment, Spectrochim. Acta A Mol. Biomol. Spectrosc. 65 (2006) 673–677, https://doi.org/10.1016/j.saa.2005.12.028.

[70] A. Mukhopadhyay, V.K. Maka, J.N. Moorthy, Remarkable influence of 'phane effect' on the excited-state properties of cofacially-oriented coumarins, Phys. Chem. Chem. Phys. 19 (2017) 4785, https://doi.org/10.1039/C6CP07720J.

[71] P. Mohammad-Jafarieh, A. Akbarzadeh, R. Salamat-Ahangari, M. Pourhassan-Moghaddam, K. Jamshidi-Ghaleh, Solvent effect on the absorption and emission spectra of carbon dots: evaluation of ground and excited state dipole moment, BMC Chemistry 15 (2021) 53, https://doi.org/10.1186/s13065-021-00779-6.

[72] Y.H. Zhao, M.H. Abraham, A.M. Zissimos, Fast calculation of van der Waals volume as a sum of atomic and bond contributions and its application to drug compounds, J. Org. Chem. 68 (2003) 7368–7373, https://doi.org/10.1021/jo034808o.

[73] C.R. Groom, I.J. Bruno, M.P. Lightfoot, S.C. Ward, The Cambridge structural database, Acta Cryst. B. 72 (2016) 171–179, https://doi.org/10.1107/S2052520616003954.